

Contents lists available at ScienceDirect

Physics Letters B

www.elsevier.com/locate/physletb $h \rightarrow \mu^+ \mu^-$ via $t\bar{t}h$ production at the LHC

Shufang Su, Brooks Thomas*

Department of Physics, University of Arizona, Tucson, AZ 85721, USA

ARTICLE INFO

Article history:

Received 24 December 2008
 Received in revised form 4 May 2009
 Accepted 17 May 2009
 Available online 20 May 2009
 Editor: B. Grinstein

ABSTRACT

In this work, we examine the process at the LHC in which a Higgs boson is produced in association with a $t\bar{t}$ pair and subsequently decays to a pair of muons. We show that the statistical significance for the discovery of a light, Standard Model Higgs boson with a mass around 120 GeV in this channel is comparable to those for other processes (gluon fusion, weak-boson fusion) in which the Higgs decays to a muon pair. Combining all three of these channels, we show that evidence for a Higgs boson with a mass in the range $115 \text{ GeV} < m_h < 130 \text{ GeV}$ could be obtained at the 3σ significance level with an integrated luminosity of 300 fb^{-1} . We also calculate the enhancement factor to the $t\bar{t}h$ cross-section that would be needed to discover a non-standard Higgs boson in this channel.

© 2009 Elsevier B.V. Open access under [CC BY license](http://creativecommons.org/licenses/by/3.0/).

1. Introduction

The CERN Large Hadron Collider (LHC) – a pp collider with center-of-mass energy $\sqrt{s} = 14 \text{ TeV}$ – will begin taking data in the very near future. One of the primary missions of the LHC is to investigate the physics behind electroweak symmetry-breaking. Since many of the most attractive candidate theories involve a Higgs sector containing one or more light, scalar degrees of freedom, a great deal of effort has been invested into determining how best to search for these scalars (and in particular the lightest CP-even scalar) at the LHC (see [1–4]). For a relatively light Higgs boson in the Standard Model (SM), with $114 \text{ GeV} \lesssim m_h \lesssim 125 \text{ GeV}$, the most favored channel is $gg \rightarrow h \rightarrow \gamma\gamma$. For a Higgs with intermediate mass $125 \text{ GeV} \lesssim m_h \lesssim 140 \text{ GeV}$, the most promising channel is the weak-boson fusion (WBF) [5] process $qq' \rightarrow qq'h (h \rightarrow \tau\tau)$ [6]. For a heavier Higgs, with $m_h \gtrsim 140 \text{ GeV}$, the channels of interest are $h \rightarrow WW^*$ and $h \rightarrow ZZ^*$, with the Higgs produced through either gluon fusion or WBF [3,4].

Clearly, additional channels which might provide evidence for a light, CP-even Higgs scalar in these mass ranges can also play a crucial role in Higgs phenomenology. This is especially true if the Higgs sector realized in nature turns out to be more complicated than the single $SU(2)$ doublet of the SM. In such cases, the most promising discovery channels could turn out to be quite different from those pertinent to a SM Higgs boson [7]. For this reason, it has become increasingly clear that channels for which the significance of discovery for a Standard Model Higgs is low may be of

crucial importance for detecting whatever variety of Higgs boson is actually out there – provided of course that nature employs a scalar Higgs sector to break the electroweak symmetry. Furthermore, if a light, CP-even Higgs boson is discovered early at the LHC, within the first $10\text{--}30 \text{ fb}^{-1}$ of data, processes which can put the most stringent bounds on parameters such as its mass, its couplings to the Standard Model fermions, etc., will become increasingly important for precision analyses of the Higgs sector that could point the way toward new physics.

One Higgs-decay channel that is of particular interest is $h \rightarrow \mu^+ \mu^-$. The primary advantage of this channel is that a signal involving a pair of high- p_T muons will be easy to identify at the LHC. Indeed, the muon-identification efficiency at the LHC detectors is more than 90% [1,2]. Once a Higgs boson is discovered in this channel, its mass could be readily reconstructed with high precision. Additionally, such a channel could be used in determining the muon Yukawa coupling. This is of particular interest because most of the existing literature on the measurement of Higgs-boson Yukawa couplings focuses on the third generation Yukawa couplings, y_b , y_τ and y_t . Consequently, $h \rightarrow \mu^+ \mu^-$ processes could be important for determining whether or not the effective Higgs Yukawa couplings are indeed generation-universal.

The difficulty with $h \rightarrow \mu^+ \mu^-$ processes is the small Higgs branching fraction into muon pairs, both in the Standard Model – in which it is of $\mathcal{O}(10^{-4})$ – and in most simple extensions of the Higgs sector. Indeed, under the assumption of universal Yukawa couplings among the lepton generations, the small size of the muon mass m_μ compared to m_τ results in $\text{BR}(h \rightarrow \mu\mu)$ being roughly two orders of magnitude smaller than $\text{BR}(h \rightarrow \tau\tau)$. Consequently, while a great deal of attention has been focused on processes in which the Higgs boson decays to a tau pair (for example, weak-boson fusion with $h \rightarrow \tau^+ \tau^-$ is now regarded as one

* Corresponding author.

E-mail addresses: shufang@physics.arizona.edu (S. Su),
brooks@physics.arizona.edu (B. Thomas).

of the promising discovery channel for the SM Higgs in the intermediate mass region [1,2,5]), $h \rightarrow \mu^+ \mu^-$ processes have not been extensively considered. Nevertheless, some parton-level studies have been carried out: investigations of $gg \rightarrow h \rightarrow \mu \mu$ and the weak-boson fusion process $qq' \rightarrow qq'h(h \rightarrow \mu \mu)$ at the LHC were performed in Refs. [8] and [9], respectively. It was found that by combining the results from both of these channels, an observation of $h \rightarrow \mu^+ \mu^-$ at the 3σ level could be obtained with 300 fb^{-1} of integrated luminosity for low Higgs masses. Higgs decays to muon pairs in the Minimal Supersymmetric Standard Model have also been studied (see, for example, Ref. [10]).

In this Letter, we examine the associated Higgs production process $t\bar{t}h$ with $h \rightarrow \mu^+ \mu^-$ at the LHC. While the rate for this process is far smaller than that for the $t\bar{t}h(h \rightarrow \tau \tau)$ channel discussed in [11], a muonic final state has a number of advantages. Perhaps the most significant of these is that the final-state muon pair affords an exceptionally good Higgs-mass resolution – of similar order (around 1%) to that afforded by $gg \rightarrow h \rightarrow \gamma \gamma$ [2,12]. In addition, the absence of any additional sources of missing energy for semileptonic top decays (beyond the single neutrino from $t \rightarrow b \ell \nu$) reduces the uncertainty in top-quark reconstruction. We show that, for a SM Higgs boson with a mass around 120 GeV, the statistical significance of discovery in the $t\bar{t}h(h \rightarrow \mu \mu)$ channel is on the same order as that obtained from the gluon fusion and WBF channels. We also investigate the prospects for detecting a SM Higgs boson via its decays to muon pairs using the combined gluon fusion, WBF, and $t\bar{t}h$ channels, and discuss the potential implications for Higgs discovery using the $t\bar{t}h(h \rightarrow \mu \mu)$ channel in beyond-the-Standard-Model scenarios.

2. Signal and backgrounds

For a SM Higgs sector, the $t\bar{t}h(h \rightarrow \mu \mu)$ channel will be useful primarily in the case where the Higgs boson is light: $114 \text{ GeV} \lesssim m_h \lesssim 140 \text{ GeV}$. (The production cross-sections drop quickly for heavier Higgs masses.) Here, we present results for the specific choices $m_h = 115 \text{ GeV}$, 120 GeV , 130 GeV , and 140 GeV . The leading-order (LO) $t\bar{t}h$ production cross-section and Higgs branching fraction to muons for each of these choices are listed in Table 1. The former were calculated using the MadGraph package [13], with factorization and renormalization scales both set to $(2m_t + m_h)/2$; the latter were calculated using HDECAY [14]. It is apparent from Table 1 that the leading-order (LO) $t\bar{t}h$ production cross-section for a Higgs boson in this mass range at the LHC ranges from around 350 to 600 fb, while the Higgs branching fraction to muons is of $\mathcal{O}(10^{-4})$, as discussed above.

Since this implies a rather small overall rate for $t\bar{t}h(h \rightarrow \mu \mu)$ events, we would like to include in our analysis all final states which permit an unambiguous reconstruction of both t and \bar{t} from their decay products. These include processes in which both W bosons decay hadronically (45.7% of the time) and semileptonic decays in which the charged lepton is either an electron or a muon (28.8% of the time). Therefore, we study two types of signals:

- (I) hadronic signatures: 6 jets + $\mu^+ \mu^-$,
- (II) semileptonic signatures: 4 jets + $\mu^+ \mu^- \ell^\pm$ + missing E_T , $\ell = e, \mu$.

For fully-leptonic $t\bar{t}$ decay, the masses of the top quarks cannot be completely reconstructed, due to the presence of multiple neutrinos in the final state. We therefore do not consider this final state in our results, but note that a more detailed analysis based on kinematical distributions as in the top-mass reconstruction methods of [1,15] could perhaps render this channel useful.

Table 1

Leading-order (LO) SM $t\bar{t}h$ production cross sections at the LHC and Higgs branching ratios to muons for several different values of the Higgs mass m_h .

m_h (GeV)	$\sigma_{t\bar{t}h}$ (fb)	BR($h \rightarrow \mu \mu$)
115	606.1	2.57×10^{-4}
120	538.1	2.40×10^{-4}
130	430.8	1.89×10^{-4}
140	347.5	1.24×10^{-4}

It may be noted that no distinction between b -jets and other jets was made in the definition of signals (I) and (II). Indeed, b -tagging is not used in this analysis and that the cuts outlined below are applied to all jets, irrespective of their b -character. The reason for this is that the b -tagging efficiency at ATLAS is around 50% [1] (the efficiency at CMS is comparable), which would lead to a substantial loss in signal events. However, we shall justify this procedure below and show that the relevant reducible backgrounds can be effectively eliminated merely by demanding that t , \bar{t} , h and both W -bosons, can all be appropriately reconstructed from the momenta of the final-state particles.

The effect of next-to-leading order (NLO) QCD corrections is incorporated in our analysis in the standard manner, via the introduction of a K -factor for each relevant signal or background process. NLO corrections to the $t\bar{t}h$ production cross-section were calculated in Ref. [16] for $m_h = 120 \text{ GeV}$. For this choice of Higgs mass, the K -factor was found to be about 1.2 at the scale $\mu = (2m_t + m_h)/2$, and was found not to vary substantially with m_h over the mass range considered here. We therefore take K_S , the K -factor for the signal process, to be equal to 1.2 for all $115 \text{ GeV} \leq m_h \leq 140 \text{ GeV}$.

The primary irreducible Standard Model background for all final states resulting from $t\bar{t}h(h \rightarrow \mu \mu)$ comes from similar processes in which the Higgs boson is replaced by an off-shell photon γ^* or a Z boson. The background was also calculated using MadGraph [13], with both the factorization and renormalization scales set to $(2m_t + m_Z)/2$. We found the tree-level cross section for $t\bar{t}Z/\gamma^*(Z/\gamma^* \rightarrow \mu \mu)$ to be 32.27 fb, where we require $p_T > 10 \text{ GeV}$ for final-state muons to keep the results well-behaved when soft photons are taken into account. This result is also modified at next-to-leading order by a K -factor, which was calculated in Ref. [17] and found to be $K_{BG} = 1.35$ at the scale $\mu = (2m_t + m_Z)/2$. Reducible backgrounds such as $bbWWZ$, also exist, but they can be eliminated by a sensible choice of cuts. In particular, mandating the successful reconstruction of the top quarks in both the hadronic channel and the semileptonic channel will render such backgrounds negligible. Therefore, in our analysis below, we only consider the irreducible background coming from $t\bar{t}Z/\gamma^*$.

We impose two sets of cuts on the signal and background data for each type of signature (hadronic or semileptonic) under consideration. The first of these sets (which we will refer to as the Level I cuts) is applied universally to all processes, and is designed to reproduce a realistic detector acceptance:

- $p_T^\ell > 20 \text{ GeV}$ for all leptons, $|\eta_\mu| < 2.4$, $|\eta_e| < 2.5$,
- $p_T^j > 15 \text{ GeV}$, $|\eta_j| < 3.0$ for all jets (including b jets),
- $\Delta R_{\ell j} > 0.4$, $\Delta R_{jj} > 0.5$, $\Delta R_{\ell \mu} > 0.5$.

Here, $\Delta R_{ab} = \sqrt{(\Delta\phi_{ab})^2 + (\Delta\eta_{ab})^2}$ denotes the ‘‘lego-plot’’ separation distance between final-state particles a and b , and p_T^a denotes the transverse momentum of a .

Reconstruction requirements underlie the second set of cuts, the specifics of which depend on the particular final states under consideration. Since the invariant mass resolution for the muon

pair will be quite good at both ATLAS [1] and CMS [2], we retain only events in which the invariant mass of some pair of muons lies within the range $|M_{\mu\mu} - m_h| < 2.5$ GeV for the particular value of m_h under consideration. In addition to this requirement, for the fully hadronic final state (I), which involves 6 jets + $\mu^+\mu^-$, we demand that some combination of jet momenta exists for which the invariant masses $M_{j_a j_b j_c}^2 = (p_{j_a} + p_{j_b} + p_{j_c})^2$ of two different sets of jets (j_a, j_b, j_c) both reconstruct a top quark. This cut is implemented primarily to reduce background contributions from processes that do not involve a top pair. Furthermore, we require that within each such set, one combination of jet momenta $M_{j_a j_b}^2 = (p_{j_a} + p_{j_b})^2$ reconstructs a W boson. Thus the full roster of Level II cuts in the fully hadronic channel comprises:

- 6 jets and 2 muons passing the Level I cuts,
- two groups of three jets each for which $|M_{j_a j_b j_c} - m_t| < 50$ GeV,
- one jet pair within each such group for which $|M_{j_a j_b} - M_W| < 40$ GeV,
- $|M_{\mu\mu} - m_h| < 2.5$ GeV.

For the semileptonic signature (II), which involves 4 jets + $\mu^+\mu^-\ell^\pm$ + missing E_T , the situation is complicated both by the presence of missing transverse momentum from the neutrino and by combinatorial issues that arise when ℓ^\pm is a muon. To address the former, we follow the standard procedure [1], which is to assume that a single neutrino produced by the leptonically-decaying top is responsible for the entirety of the missing momentum in the transverse plane and that $M_W^2 = (p_\nu + p_\ell)^2$. Under this assumption, one can solve for the longitudinal component p_ν^z of the neutrino momentum up to a sign ambiguity. Of the two resulting solutions for p_ν^z , we select the one with the larger absolute value and use it to reconstruct a mass for the leptonically-decaying top. For final states involving at least one electron, we then require that there exist one jet and one electron which, in this manner, reconstruct m_t to within 50 GeV. For final states that contain at least three muons, we accept any event for which there exists some combination of muons which reconstructs both m_h and m_t successfully according to the method outlined above, provided that the muons used to reconstruct the Higgs mass have opposite sign. However since combinatorial issues of this sort can have a pronounced effect when the primary background is associated with the tail of a kinematical distribution, far away from the Z -pole, we apply a more stringent constraint in this case and require that m_t be reconstructed within 10 GeV. To reconstruct the remaining top quark, we use the same method employed in the fully-hadronic case: we require that there exist one combination of three other jets whose invariant mass reconstructs m_t within 50 GeV, two of which reconstruct M_W within 40 GeV.

To recapitulate, then, the Level II cuts for the semileptonic case are:

- 4 jets and 3 charged leptons (at least two of which are muons) passing the Level I cuts,
- a groups of three jets each for which $|M_{j_a j_b j_c} - m_t| < 50$ GeV,
- one jet pair within this group for which $|M_{j_a j_b} - M_W| < 40$ GeV,
- 2 opposite-sign muons for which $|M_{\mu\mu} - m_h| < 2.5$ GeV,
- one additional electron and one additional jet for which $|M_{j_e \nu} - m_t| < 50$ GeV, or one additional muon and one additional jet for which $|M_{j_{\mu\nu}} - m_t| < 10$ GeV,

where the neutrino four-momentum is reconstructed in the manner discussed above. Note that the process in which the charged lepton from the leptonically-decaying top is a muon and the pro-

Table 2

Signal and background results for $t\bar{t}h(h \rightarrow \mu\mu)$ in the fully hadronic channel for several different values of m_h . The signal and background efficiencies ϵ_S and ϵ_B (including the top quark decay branching ratios) associated with the combined Level I and Level II cuts described in the text are displayed here, along with the signal and background cross-sections (in ab) after all cuts have been applied. The cross sections quoted here include the relevant NLO K -factors for both signal and background processes. The Gaussian-equivalent statistical significance (see text for further explanation) is also given for 300 fb^{-1} of integrated luminosity at both ATLAS and CMS, along with the result for S/B .

m_h (GeV)	ϵ_S	σ_S (ab)	ϵ_B	σ_B (ab)	S/B	Significance $\mathcal{L} = 300 \text{ fb}^{-1}$
115	8.1%	15.1	0.028%	12.3	1.22	2.66
120	7.9%	12.2	0.023%	10.0	1.21	2.36
130	8.2%	8.0	0.017%	7.3	1.10	1.81
140	8.2%	4.2	0.015%	6.6	0.64	0.81

cess in which it is an electron represent two distinct channels with different backgrounds, detection efficiencies, etc. These results pertaining to these channels will thus be reported separately.

3. Results

The results of our analysis of $t\bar{t}h(h \rightarrow \mu\mu)$ in the hadronic and semileptonic channels are displayed in Tables 2 and 3, respectively. The respective efficiencies ϵ_S and ϵ_B of the cuts discussed above in reducing the number of signal and background events in each case are shown, along with cross-sections for the corresponding processes which include the effect of these efficiencies. Note that here we have defined ϵ_S and ϵ_B for each channel to include the branching fraction of $t\bar{t}$ to the corresponding final state. In addition, signal-to-background ratios S/B and statistical significances are also displayed. Due to the small background event counts obtained at $\mathcal{O}(300 \text{ fb}^{-1})$ luminosities, all confidence levels were computed using Poisson statistics, for which $\text{CL}_{\text{Pois}} = 1 - p$, where p is the p -value in question. The $t\bar{t}h(h \rightarrow \mu\mu)$ significance numbers quoted in this work are those which would correspond to an equivalent confidence level for a Gaussian distribution, for which $\text{CL}_{\text{Gauss}} = 1 - 2p$. Signal and background events for each process were generated using the MadEvent package [13] and processed using PYTHIA [18]. The generated events were then passed through PGS4 [19] for detector simulation. A total of 40,000 events were simulated for the signal process; for the background process, on which the effect of the cuts is more severe, ten times that number were simulated in order to limit the effect of statistical fluctuations.

The hadronic channel gives the best statistical significance for $t\bar{t}h(h \rightarrow \mu\mu)$. We find that evidence for a light ($m_h = 115$ GeV) SM Higgs boson may be obtained at the 2.66σ significance level with 300 fb^{-1} of integrated luminosity at both ATLAS and CMS. The statistical significance of this channel decreases with increasing Higgs mass, primarily due to the decrease both in the $t\bar{t}h$ production cross-section and in the branching ratio of Higgs decay to muons. This notwithstanding, for all $115 \text{ GeV} < m_h < 140 \text{ GeV}$, the signal cross-section for this process is large enough that a reasonable number of signal events can be expected at such luminosities.

By contrast, the semileptonic channels are slightly less promising, primarily because the efficiency factor ϵ_S is significantly smaller than in the fully-hadronic channel. Furthermore, a much larger fraction of background events survive the cuts in the channel in which the charged lepton produced by the leptonically-decaying top is a muon than in the channel where it is an electron. Taking into account the contributions from both of these final states, we find that with 300 fb^{-1} of integrated luminosity at both ATLAS and CMS, semileptonic $t\bar{t}h$ events can provide evidence at the 0.96σ significance level for a light ($m_h = 115$ GeV) Higgs boson.

Table 3

Signal and background results for $t\bar{t}h(h \rightarrow \mu\mu)$, with $t\bar{t} \rightarrow 2 \text{ jets} + \ell^\pm + \text{missing } E_T$, for both $\ell = e$ and $\ell = \mu$, are shown here for several different values of m_h , including all relevant K -factors, etc. For further explanation of the notation, see the caption for Table 2. The combined statistical significance in the semileptonic channel from both contributions for $\mathcal{L} = 300 \text{ fb}^{-1}$ is also supplied.

m_h (GeV)	$W \rightarrow e\nu_e$					$W \rightarrow \mu\nu_\mu$					Significance ($\mathcal{L} = 300 \text{ fb}^{-1}$)
	ϵ_S	$\sigma_S(ab)$	ϵ_B	$\sigma_B(ab)$	S/B	ϵ_S	$\sigma_S(ab)$	ϵ_B	$\sigma_B(ab)$	S/B	
115	1.6%	3.0	0.0045%	1.9	1.55	0.74%	1.4	0.011%	5.0	0.28	0.96
120	1.8%	2.7	0.0025%	1.1	2.51	0.70%	1.1	0.013%	5.4	0.20	0.77
130	1.7%	1.7	0.0030%	1.3	1.26	0.76%	0.7	0.010%	4.4	0.17	0.48
140	1.7%	0.9	0.0013%	0.5	1.63	0.74%	0.4	0.008%	3.4	0.11	0.07

Table 4

Combined statistical significance for $t\bar{t}h(h \rightarrow \mu\mu)$ ($t\bar{t}h_{\text{comb}}$) and significance in the hadronic channel alone ($t\bar{t}h_{\text{had}}$) in the Standard Model, displayed alongside those for gluon fusion [8] and weak-boson fusion [9] processes in which the Higgs boson decays to $\mu^+\mu^-$. The significance values quoted here correspond to $\mathcal{L} = 300 \text{ fb}^{-1}$ for both ATLAS and CMS.

m_h (GeV)	Significance				Significance (GF + WBF)	Combined
	$t\bar{t}h_{\text{comb}}$	$t\bar{t}h_{\text{had}}$	GF	WBF		
115	2.43	2.66	2.41	2.49	3.37	4.04
120	2.02	2.36	2.51	2.52	3.45	3.94
130	1.43	1.81	2.25	2.40	3.18	3.41
140	0.38	0.81	1.61	1.71	2.26	2.09

Table 5

The integrated luminosity needed to claim a 3σ or 5σ discovery of the Standard Model Higgs boson at the LHC in the hadronic $t\bar{t}h(h \rightarrow \mu\mu)$ channel for a several different choices of m_h . The luminosity needed to claim a 3σ or 5σ discovery using the combined gluon fusion, weak-boson fusion, and hadronic $t\bar{t}h$ Higgs production channels, with $h \rightarrow \mu^+\mu^-$, is also shown.

m_h (GeV)	$t\bar{t}h$		$t\bar{t}h + \text{GF} + \text{WBF}$	
	$\mathcal{L}^{3\sigma}$ (fb^{-1})	$\mathcal{L}^{5\sigma}$ (fb^{-1})	$\mathcal{L}^{3\sigma}$ (fb^{-1})	$\mathcal{L}^{5\sigma}$ (fb^{-1})
115	339	924	174	430
120	417	1138	192	440
130	669	1875	245	571
140	2008	5563	485	1270

Since the signal cross-sections are relatively small for both contributing channels, however, with σ_S of $\mathcal{O}(ab)$ after all cuts have been applied, only a small number of surviving events will be produced at such luminosities – at least for a Standard Model Higgs boson.

In Table 4, we present the combined $t\bar{t}h$ results from both hadronic and leptonic channels. These combined significances, obtained by combining the p -values for the individual (Poisson) processes via Fisher's method, are smaller than those for the hadronic channel alone (also displayed), due to the relatively low confidence levels for each of the two semileptonic channels. It will therefore be advantageous henceforth to focus on the results in the hadronic $t\bar{t}h$ channel alone. We have also listed the significances for $gg \rightarrow h \rightarrow \mu\mu$ [8] and $qq' \rightarrow qq'h(h \rightarrow \mu\mu)$ [9] in Table 4 for comparison. Note that the significances quoted for these processes, which obey Gaussian statistics, are given by S/\sqrt{B} . For a SM Higgs mass around 115 GeV, the statistical significance in the (hadronic) $t\bar{t}h(h \rightarrow \mu\mu)$ channel is similar to or even higher than that in the other two channels. With $\mathcal{L} = 300 \text{ fb}^{-1}$, we observe that a statistical significance of 4.04σ may be obtained by combining the results from all three channels. This represents a substantial increase over the 3.37σ obtained from considering the gluon-fusion and WBF processes alone. In Table 5, we presented the integrated luminosity at the LHC that is needed for a 3σ and 5σ discovery with hadronic $t\bar{t}h(h \rightarrow \mu\mu)$ alone, and with all three production processes ($t\bar{t}h$, gluon-fusion, WBF) included. For a Higgs boson just slightly heavier than the LEP bound of 114 GeV [20], a 3σ discovery can be obtained with around 170 fb^{-1} of integrated luminosity.

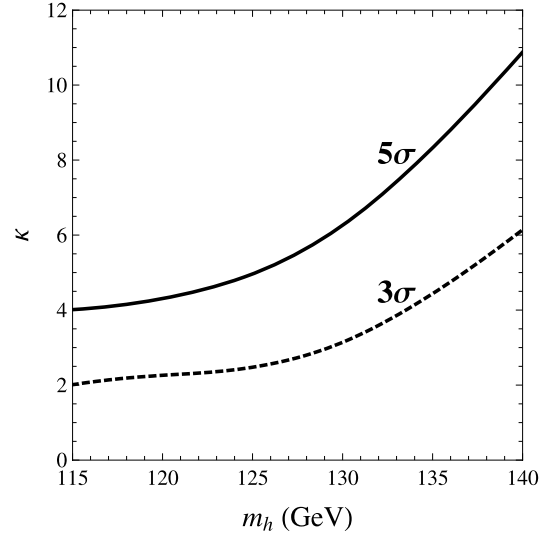


Fig. 1. Plot of the enhancement factor κ – see Eq. (1) – necessary to obtain evidence for a light, non-standard CP-even Higgs boson at the 3σ or 5σ level at LHC with $\mathcal{L} = 100 \text{ fb}^{-1}$ at both ATLAS and CMS, given as a function of the Higgs boson mass m_h . The dotted line corresponds to a 3σ effect, whereas the solid line corresponds to a 5σ effect.

We have shown that the $t\bar{t}h(h \rightarrow \mu\mu)$ channel can provide 2.66σ evidence for a light, SM Higgs boson around 115 GeV. In non-Standard Model Higgs scenarios, however, the branching ratio for $h \rightarrow \mu^+\mu^-$ and/or $t\bar{t}h$ production cross section might potentially be enhanced, rendering this channel even more significant for Higgs-boson detection. Depending on the enhancement factor, a 5σ discovery might even be possible – and at a reasonably low integrated luminosity. In order to quantify these effects, we define an overall enhancement factor κ , which represents the net effect of all modifications to $\text{BR}(h \rightarrow \mu\mu)$ and the $t\bar{t}h$ production cross-section in a given extension of the SM Higgs sector:

$$\kappa \equiv \frac{[\sigma(pp \rightarrow t\bar{t}h) \times \text{BR}(h \rightarrow \mu\mu)]_{NP}}{[\sigma(pp \rightarrow t\bar{t}h) \times \text{BR}(h \rightarrow \mu\mu)]_{SM}}. \quad (1)$$

Fig. 1 shows the enhancement factor κ as a function of Higgs mass for a 3σ or 5σ discovery at the LHC with 100 fb^{-1} of integrated luminosity at both ATLAS and CMS. For values of m_h in the range $115 \leq m_h \lesssim 130 \text{ GeV}$, an enhancement factor of $\kappa \gtrsim 2$ –3 (depending on m_h) is sufficient to result in a 3σ excess, while $\kappa \gtrsim 4$ –6 will result in a 5σ excess in the combined $t\bar{t}h(h \rightarrow \mu\mu)$ channels and the clear discovery of a beyond-the-Standard Model Higgs boson.

4. Conclusions

In this Letter, we have investigated the observability of a light, CP-even Higgs boson at the LHC in the channel $t\bar{t}h(h \rightarrow \mu\mu)$. We have shown that for a light SM Higgs boson with a mass around

120 GeV, evidence for a Standard Model Higgs can be obtained in this channel at roughly the same significance level as in the $gg \rightarrow h \rightarrow \mu\mu$ and $qq' \rightarrow qq'h(h \rightarrow \mu\mu)$ channels, and with comparable Higgs-mass resolution. The best statistical significance is obtained in the fully hadronic mode. Moreover, we have shown that for m_h between 115 GeV and 130 GeV, the combined results from the gluon-fusion, weak-boson fusion, and $t\bar{t}h$ channels, with h decaying to $\mu^+\mu^-$, can provide evidence for a SM Higgs boson at about 3σ or better with 300 fb^{-1} of integrated luminosity. In beyond-the-Standard Model scenarios in which the $t\bar{t}h$ production cross-section and/or the branching fraction $\text{BR}(h \rightarrow \mu\mu)$ are enhanced relative to their SM values, this channel could become extremely important for the detection and analysis of a light Higgs boson, providing an accurate measurement of the Higgs mass, and a precise determination of the muon Yukawa coupling.

Acknowledgements

We wish to thank A. Belyaev, T. Han, B. McElrath, and M. Schmitt for correspondence and discussion. We also wish to thank the Institute for Nuclear Theory at the University of Washington for its hospitality and the Department of Energy for partial support during the completion of this work. This work was supported in part by the Department of Energy under Grant DE-FG02-04ER-41298.

References

- [1] ATLAS detector and physics performance. Technical design report, vol. 2, ATLAS Collaboration, ATLAS-TDR-15; CERN-LHCC-99-015.
- [2] G.L. Bayatian, et al., CMS Collaboration, J. Phys. G 34 (2007) 995.
- [3] S. Asai, et al., Eur. Phys. J. C 32S2 (2004) 19, arXiv:hep-ph/0402254.
- [4] S. Abdullin, et al., Eur. Phys. J. C 39S2 (2005) 41.
- [5] D.L. Rainwater, D. Zeppenfeld, JHEP 9712 (1997) 005, arXiv:hep-ph/9712271.
- [6] D.L. Rainwater, D. Zeppenfeld, K. Hagiwara, Phys. Rev. D 59 (1999) 014037, arXiv:hep-ph/9808468.
- [7] See, for example, D. Phalen, B. Thomas, J.D. Wells, Phys. Rev. D 75 (2007) 117702, arXiv:hep-ph/0612219; S. Mantry, M.J. Ramsey-Musolf, M. Trott, Phys. Lett. B 660 (2008) 54, arXiv:0707.3152 [hep-ph]; W.D. Goldberger, B. Grinstein, W. Skiba, Phys. Rev. Lett. 100 (2008) 111802, arXiv:0708.1463 [hep-ph]; S. Mantry, M. Trott, M.B. Wise, Phys. Rev. D 77 (2008) 013006, arXiv:0709.1505 [hep-ph]; L. Randall, JHEP 0802 (2008) 084, arXiv:0711.4360 [hep-ph]; J. Fan, W.D. Goldberger, A. Ross, W. Skiba, arXiv:0803.2040 [hep-ph].
- [8] T. Han, B. McElrath, Phys. Lett. B 528 (2002) 81, arXiv:hep-ph/0201023.
- [9] T. Plehn, D.L. Rainwater, Phys. Lett. B 520 (2001) 108, arXiv:hep-ph/0107180.
- [10] V.D. Barger, C. Kao, Phys. Lett. B 424 (1998) 69, arXiv:hep-ph/9711328; S. Dawson, D. Dicus, C. Kao, Phys. Lett. B 545 (2002) 132, arXiv:hep-ph/0208063; S. Dawson, D. Dicus, C. Kao, R. Malhotra, Phys. Rev. Lett. 92 (2004) 241801, arXiv:hep-ph/0402172.
- [11] A. Belyaev, L. Reina, JHEP 0208 (2002) 041, arXiv:hep-ph/0205270.
- [12] L. Carminati, ATLAS Collaboration, Acta Phys. Pol. B 38 (2007) 747.
- [13] J. Alwall, et al., JHEP 0709 (2007) 028, arXiv:0706.2334 [hep-ph].
- [14] A. Djouadi, J. Kalinowski, M. Spira, Comput. Phys. Commun. 108 (1998) 56, arXiv:hep-ph/9704448.
- [15] V. Simak, P. Homola, J. Valenta, R. Leitner, ATL-PHYS-2001-018; I. Borjanovic, et al., Eur. Phys. J. C 39S2 (2005) 63, arXiv:hep-ex/0403021.
- [16] W. Beenakker, S. Dittmaier, M. Kramer, B. Plumper, M. Spira, P.M. Zerwas, Phys. Rev. Lett. 87 (2001) 201805, arXiv:hep-ph/0107081; S. Dawson, C. Jackson, L.H. Orr, L. Reina, D. Wackerroth, Phys. Rev. D 68 (2003) 034022, arXiv:hep-ph/0305087.
- [17] A. Lazopoulos, T. McElmurry, K. Melnikov, F. Petriello, arXiv:0804.2220 [hep-ph].
- [18] T. Sjostrand, S. Mrenna, P. Skands, JHEP 0605 (2006) 026, arXiv:hep-ph/0603175.
- [19] PGS – Pretty Good Simulator, <http://www.physics.ucdavis.edu/~conway/research/software/pgs/pgs4-general.html>.
- [20] LEP Higgs Working Group, ALEPH Collaboration, DELPHI Collaboration, arXiv:hep-ex/0107030.